Chemical Engineering Journal 153 (2009) 101–107

Contents lists available at ScienceDirect

Chemical Engineering Journal

journal homepage: www.elsevier.com/locate/cej

As(III) removal from drinking water using manganese oxide-coated-alumina: Performance evaluation and mechanistic details of surface binding

Shihabudheen M. Maliyekkal[a], Ligy Philip[a,*], T. Pradeep[b,1]

[a] EWRE Division, Department of Civil Engineering, Indian Institute of Technology, Madras, Chennai 600036, India
[b] Department of Chemistry and Sophisticated Analytical Instruments Facility, Indian Institute of Technology, Madras, Chennai 600036, India

ARTICLE INFO

Article history:
Received 14 June 2008
Received in revised form 2 June 2009
Accepted 16 June 2009

Keywords:
Adsorption
Arsenite
Drinking water
Manganese oxide-coated-alumina
Raman spectroscopy

ABSTRACT

This paper describes the arsenite [As(III)] removal performance of manganese oxide-coated-alumina (MOCA) and its interaction with As(III) in drinking water. MOCA was characterized by XRD, SEM, EDAX, gas adsorption porosimetry, and point of zero charge (pH_{pzc}) measurements. Raman spectroscopy coupled with sorption experiments were carried out to understand the As(III) interaction with MOCA. As(III) sorption onto MOCA was pH dependent and the optimum removal was observed between a pH of 4 and 7.5. The Sips isotherm model described the experimental equilibrium data well and the predicted maximum As(III) sorption capacity was 42.48 mg g^{-1}, which is considerably higher than that of activated alumina (20.78 mg g^{-1}). The sorption kinetics followed a pseudo-second-order equation. Based on sorption and spectroscopic measurements, the mechanism of As(III) removal by MOCA was found to be a two-step process, i.e. oxidation of As(III) to arsenate (As(V)) and retention of As(V) on MOCA surface, with As(V) forming an inner surface complex with MOCA. The results of this study indicated that MOCA is a promising alternative sorbent for As(III) removal from drinking water.

1. Introduction

The removal of dissolved arsenic from drinking water has been a great challenge to environmental engineers because of its ubiquity and multiple impacts on human health. The intricate aqueous chemistry of arsenic made this task more challenging. Arsenate (H_3AsO_4, $H_2AsO_4^-$, $HAsO_4^{2-}$) and arsenite (H_3AsO_3, $H_2AsO_3^-$, $HAsO_3^{2-}$) are the two major arsenic species generally found in the groundwater system [1]. Arsenite [As(III)] is generally more toxic and predominant in many affected groundwaters [2–4].

There are many treatment technologies existing for the removal of arsenic from drinking water system. However, all of these treatment technologies are successful for As(V), but fall short in the case of As(III) [5,6]. Adsorption as a treatment methodology has been receiving increasing attention for arsenic removal in small scale water treatment systems because of its simplicity and versatility in operation. Granular activated alumina (AA) is reported to be the best demonstrated sorbent for removing arsenic from drinking water [7,8]. However, the slow rate of adsorption as well as low adsorption capacity for As(III) limits the use of AA in treating large quantities of As(III) contaminated groundwater. Consequently, pre-oxidation of As(III) to As(V) is always preferred to enhance the removal efficiency. Many oxidants or oxidant-generating systems, including chlorine, manganese oxides, ozone, UV irradiation with (TiO_2/UV) and many others have been tested for the oxidation of As(III) [5,9–10]. However, introducing a pre-oxidation step increases the complexity and reduces the overall viability of operation in small scale house-hold treatment units. The cost and chance of side reaction with natural organic matter also limits the use of powerful oxidizing agents like TiO_2/UV, ozone and hydrogen peroxide. The drawback in using chlorine is that it will react with natural organic matter to form chlorinated by-products that are harmful to health.

Recently, many metal oxides including iron and manganese have been tested for As(III) removal. It is reported that manganese oxides can effectively oxidize As(III) and have good ability to adsorb As(V) [11–13]. But, most of these metal oxides are available only as fine powders or are generated in aqueous suspension, like hydroxides or gels [14]. Adsorbents in powder form have practical limitations, including difficulty in solid/liquid separation, low hydraulic conductivity and leaching of the metal/metal oxide along with treated water. To overcome these limitations, manganese oxide can be immobilized on activated alumina surface. This kind of alumina-supported manganese oxide catalyst has been widely known for its oxidation reactions of various compounds. The application of such media for the oxidation and simultaneous removal of As(III) from drinking water is not much explored. Recently, Kunzru and Chaudhuri [15] demonstrated the superiority of manganese amended

* Corresponding author. Fax: +91 44 2254252.
E-mail addresses: shihab@iitm.ac.in (S.M. Maliyekkal), ligy@iitm.ac.in (L. Philip), pradeep@iitm.ac.in (T. Pradeep).
[1] Fax: +91 44 2257 0509x0545.

1385-8947/$ – see front matter © 2009 Elsevier B.V. All rights reserved.
doi:10.1016/j.cej.2009.06.026

Nomenclature

C_e	equilibrium concentration of the sorbate in the solution ($mg\,l^{-1}$)
q_e	amount of sorbate removed from aqueous solution at equilibrium ($mg\,g^{-1}$)
q_t	amount of adsorbate sorbed on the sorbent surface at any time, t ($mg\,g^{-1}$)
q_{cal}	calculated solid phase sorbate concentration ($mg\,g^{-1}$)
q_{exp}	experimentally measured solid phase sorbate concentration ($mg\,g^{-1}$)
k_1	first-order rate constant of sorption (h^{-1})
k_2	second-order rate constant of sorption ($g\,mg^{-1}\,h^{-1}$)
K_p	constant of intraparticle diffusion ($g\,mg^{-1}\,h^{-1/2}$)
t	reaction time (h)
x	mass of solute sorbed on the sorbent ($mg\,l^{-1}$)
m	mass of adsorbent (g)
K_F	Freundlich isotherm constant ($mg\,g^{-1}$) ($mg\,l^{-1}$)$^{-1/n}$
K_S	Sips isotherm constant ($l\,g^{-1}$)
q_{mL}	monolayer capacity of Langmuir equation ($mg\,g^{-1}$)
q_{mS}	specific sorption capacity of Sips equation at saturation ($mg\,g^{-1}$)
n	Freundlich isotherm exponent
b_L	Langmuir isotherm constant ($l\,mg^{-1}$)
m_S	Sips isotherm exponent

activated alumina (MAA) over AA in removing arsenic from drinking water. No information is available on the performance of this material under various operating and environmental conditions. Besides, to the best of our knowledge, no attempts have been made so far to understand the mechanism of As(III) sorption onto manganese oxide-coated-alumina (MOCA).

Present study evaluated the As(III) removal potential of MOCA under various operating conditions such as pH, ionic strength, co-existing anions, and initial As(III) concentrations. The surface arsenic species present on MOCA, the possible leaching of Mn(II) solution and the kinetics associated with As(III) removal are investigated in detail. The physicochemical characteristics of MOCA were examined with X-ray diffraction (XRD), scanning electron microscopy (SEM), energy dispersive analysis of X-rays (EDAX), gas adsorption porosimetry, Raman spectroscopy, and point of zero charge (pH_{pzc}) measurements.

2. Materials and methods

2.1. Chemicals

Chemicals used in this study were of analytical grade. They were procured from Ranbaxy Fine Chemical Limited, Chennai, India. Atomic absorption standard solution of 1000 $\mu g\,ml^{-1}$ was obtained from J.T. Backer, U.S.A. Arsenite stock solution of 1000 $mg\,l^{-1}$ was prepared from sodium arsenite ($NaAsO_2$ J.T. Backer, U.S.A.) using distilled water.

2.2. Adsorbent

AA (grade = AD101-F, cost ~1.5 $/kg) was procured from ACE Manufacturing and Marketing, Baroda, India. MOCA preparation was carried out in two steps. In step one, 25 g of AA was impregnated with 25 ml of 1.5 M $(CH_3COO)_2Mn$ in a heat resistant dish and the mixture was heated to 110 °C after thorough mixing, until it became dry. In step two, the same mixture was calcined at 400 °C for 3 h, cooled to room temperature and washed with distilled water until the washed water became clear. The washed samples were dried (110 °C for 8 h) and stored in airtight containers for further use. The cost of the prepared sorbent was estimated to be ~2.6 $/kg.

2.3. Material characterization

Manganese impregnated on the AA was quantified by acid digestion method suggested by the National Environment Protection Council [16]. Mineral phases of the manganese oxide coating were characterized by powder XRD (PANalytical X'pert PRO). EDAX (FEI, Quanta 200) was used to confirm the existence of manganese on the surface of MOCA. Analysis of physical characteristics (specific surface area, pore size and micropore volume) of MOCA and AA was measured with nitrogen adsorption isotherm technique with a micropore analyzer (ASAP 2020, Micromeritics, U.S.A.). pH_{pzc} of MOCA and AA were determined by the batch equilibrium method [17]. Raman spectra of the virgin and As(III) sorbed samples were obtained using a WiTec confocal Raman spectrometer (GmbH, Alpha-SNOM CRM 200). The excitation source used was an Ar ion laser of 514.5 nm wavelength. The Raman signal was collected in a back-scattering geometry after passing through a super-notch filter. A peltier cooled charge coupled device (CCD) was used as the detector and the signal was dispersed using an 1800 grooves/mm grating.

2.4. Batch sorption experiments

Batch sorption experiments were conducted to study the effect of contact time, initial As(III) concentration, pH, ionic strength and type and concentration of various co-existing ions on As(III) sorption by MOCA and AA. Each experiment was performed with dry sorbent dose of 5 $g\,l^{-1}$. Adsorbent samples were added to 250 ml Erlenmeyer flasks containing 100 ml of synthetic As(III) solution. The flasks were kept for shaking at 90 rpm in a thermostatically controlled orbital shaker (Remi, India) at 30 ± 1 °C. Samples were withdrawn at predetermined time intervals and analyzed for residual As(III) concentrations. The initial pH of the samples was adjusted using dilute NaOH or HCl.

Effects of contact time and initial As(III) concentration on sorption were tested with four different As(III) concentrations (0.95, 2.4, 4.9 and 9.98 $mg\,l^{-1}$). Samples were withdrawn from the reactor at small time intervals and analyzed for residual arsenic concentration. Isotherm studies were performed at pH 7.0 (±0.2) and temperature 30 °C (±1 °C). The initial concentrations of the As(III) solution were varied over a wide range (2–300 $mg\,l^{-1}$). The effect of pH on As(III) sorption was determined by varying the pH from 4 to 10. The effect of ionic strength on As(III) sorption was performed by varying the background electrolyte (NaCl) concentration over a range of 0–0.5 M.

Samples for Raman spectroscopic analysis were prepared by reacting 1 g of MOCA with 25 ml of 0.1 M As(III) at a pH of 6 or 8. A background electrolyte concentration of 0.1 M NaCl was maintained in all the samples. After equilibrating the sorbent with As(III) solution, they were separated, washed with de-ionized water, and freeze dried. They were analyzed with the spectrometer.

2.5. Analytical methods

The concentrations of total arsenic and manganese were measured using an atomic absorption spectrophotometer (PerkinElmer, AA analyst 700, U.S.A.) with a graphite furnace and an electrodeless discharge lamp (EDL). Arsenic analysis was carried out at a wavelength of 193.7 nm, slit width producing a wave band of 0.7 l nm. An Expandable Ion Analyzer (EA 940, Thermo Orion, U.S.A.) was used to measure pH of the liquid samples.

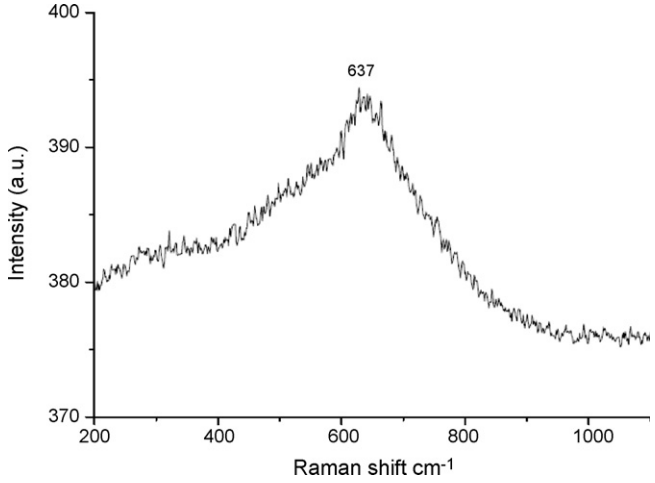

Fig. 1. Raman spectrum of MOCA before reacting with As(III).

3. Results and discussion

3.1. Material characterization studies

The quantification of manganese by acid digestion method showed it to be 5–6% of the AA support. Surface mineralogy of manganese oxide-coated-alumina was tested by powder XRD (figure not shown). The activated alumina mineralogy was identified as $Al_{21.333}O_{32}$ [Joint Committee on Powder Diffraction Standards (JCPDS) -80-0955]. No specific crystalline manganese oxide peaks were observed in XRD. The absence of manganese oxide peaks was attributed to the higher dispersion of supported manganese oxide phase or relatively low concentration of the coated manganese oxide. Kapteijin et al. [18] have also reported a similar observation. According to their finding, alumina-supported manganese oxide catalyst prepared by Mn-acetate had higher dispersion and poor crystalline structure. For further investigation and comparison, a Raman spectrum of MOCA was taken and is presented in Fig. 1. MOCA exhibited a broad Raman band at 637 cm^{-1}, which is also in agreement with the observation made by Kapteijin et al. [18]. Malinger et al. [19] reported that Raman band at 630–640 cm^{-1} can be attributed to MnO_2.

Physical surface characteristics, such as specific surface area, micropore volume, and pore size distributions of MOCA and AA are given in Table 1. The SEM micrographs of MOCA and AA are presented in Fig. 2. A clear difference in the surface morphology was observed for MOCA from AA. SEM image of AA has shown a distinct crystalline pattern with hexagonal morphology whereas, MOCA shows many aggregated small particles. The EDAX analysis of MOCA (Fig. 3) showed the signals corresponding to Al, Mn, and O, which is an indirect evidence of the existence of manganese oxide on the surface of AA.

Table 1
Physical characteristics of AA and MOCA.

Physical characteristics	AA	MOCA
Particle size	0.5–0.6 mm	0.5–0.6 mm
Shape	Spherical	Spherical
BET surface area ($m^2\ g^{-1}$)	242.07 $m^2\ g^{-1}$	194.09 $m^2\ g^{-1}$
BJH adsorption cumulative volume of pores between 17,000 Å and 3,000,000 Å diameter	0.299 $cm^3\ g^{-1}$	0.250 $cm^3\ g^{-1}$
BJH desorption cumulative volume of pores between 17,000 Å and 3,000,000 Å diameter	0.306 $cm^3\ g^{-1}$	0.283 $cm^3\ g^{-1}$
BJH desorption average pore diameter (4 V/A)	59.71 Å	47.22 Å

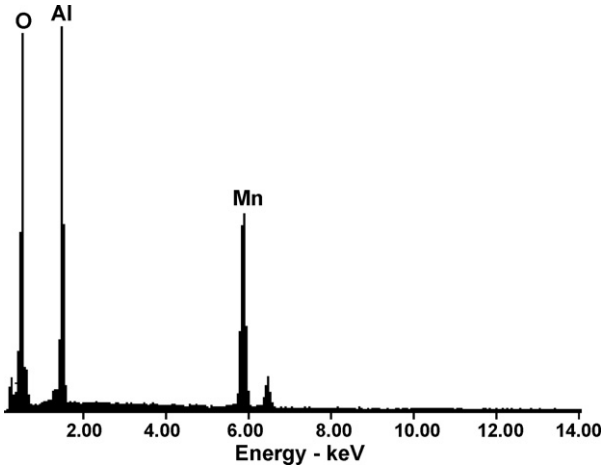

Fig. 3. EDAX spectrum of as synthesized MOCA (before reacting with As(III)).

The value of pH_{pzc} obtained for AA and MOCA is 8.25 ± 0.2 and 7.5 ± 0.2, respectively. No pH_{pzc} values were reported in the literature for MOCA prepared as earlier. Hence, it is difficult to compare this value with other literature values. Different pH_{pzc} values ranging from 8.4 to 9 were reported for different types of alumina. However, these values were obtained by different methods by various investigators and these numbers are not necessarily comparable [20].

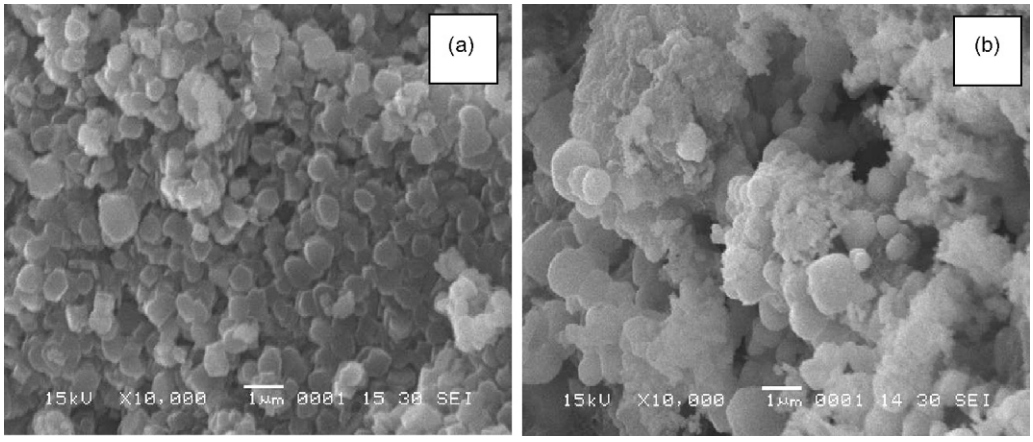

Fig. 2. SEM micrograph of AA (a) and MOCA (b) before reacting with As(III).

3.2. Batch sorption studies

3.2.1. Sorption kinetic studies

Sorption kinetic studies were conducted with MOCA and AA in batch mode. Fig. 1a and b of the supplementary data depicts the kinetics of As(III) sorption onto MOCA and AA at various initial concentrations, respectively. From these figures, it is observed that adsorption of As(III) onto MOCA is much faster than that onto AA. For an initial concentration of 1000 μg l^{-1}, MOCA could remove most of the As(III) from the aqueous system in a time period of 2–3 h. However, AA took 10 h of contact time to remove 78% of As(III). For higher concentrations, adsorption process prolonged up to 10 h to reach a pseudo-equilibrium value, for both AA and MOCA.

The analysis of sorption kinetics of As(III) onto MOCA and AA were carried out using different models. Lagergren pseudo-first-order model [21] and Ho's pseudo-second-order reaction rate models [22] have been employed to describe the kinetic process. Mathematical representations of these models are given in Eqs. (1) and (2), respectively.

Pseudo-first-order equation:

$$q_t = q_e(1 - e^{-k_1 t}) \quad (1)$$

Ho's pseudo-second-order equation:

$$q_t = \frac{q_e^2 k_2 t}{1 + q_e k_2 t} \quad (2)$$

where amount of adsorbate sorbed on the sorbent surface at any time, t (mg g^{-1}); q_e is the amount of adsorbate removed from aqueous solution at equilibrium (mg g^{-1}); k_1 is the first order rate constant of sorption (h^{-1}); k_2 is the second-order rate constant of sorption (g mg^{-1} h^{-1}); and t is the time (h).

Linear regression methods are the commonly used technique for determining the best fitting models. However, non-linear methods offer a better way to obtain the kinetic parameters since they do not alter the error structure, error variance and normality assumption of the standard least square. In the present study, non-linear method was used to find the best fitting model and kinetic parameters, which were found by trial and error methods by means of Microsoft Excel®) software using *solver* add-in option [23]. The objective function (OF) used to minimize error is given below:

$$\mathrm{OF} = \sum_{i}^{n} (q_{e,i} - q_{p,i})^2 \quad (3)$$

Fig. 4 shows the pseudo-second-order kinetic model fits for adsorption of As(III) onto MOCA (Fig. 2 in the supplementary data depicts the corresponding graph for AA, pseudo-first-order plots are not shown for brevity). Suitability of the model to fit the experimental data was examined based on root mean square error (RMSE) values. The smaller RMSE value indicates better curve fitting. Tables 2 and 3 represent the first-order and second-order rate constants obtained for As(III) sorption on to MOCA and AA, respectively. From these results, it is observed that both models have predicted the data fairly well. However, relatively lower RMSE value was observed for the pseudo-second-order kinetic model, especially for As(III) sorption onto MOCA.

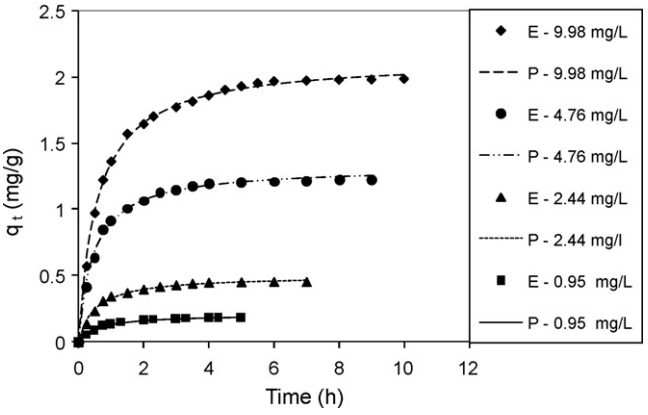

Fig. 4. Pseudo-second-order plots for As(III) removal by MOCA at various initial As(III) concentrations.

For any porous material, especially in an agitated system, the main resistance to mass transfer occurs during the movement or diffusion of solute within the pores of the particles. Axe and Trivedi [24] showed that intraparticle surface diffusion was the rate limiting process for metal ion adsorption by microporous metal oxides in aquatic and soil environment. To test the contribution of intraparticle diffusion on the adsorption process, the rate constant for intraparticle diffusion was calculated using Eq. (4) [25]:

Intraparticle diffusion model:

$$q_t = K_p t^{1/2} \quad (4)$$

For calculating the intraparticle diffusion coefficient, K_p, a plot of q_t against square root of time, $t^{1/2}$was made. K_p values were calculated from the slope of the plot. From these values, it was observed that intraparticle diffusion plays a significant role in the adsorption process. However, the linear portion of the curves (not shown for the sake of brevity) did not pass through the origin for both AA and MOCA, indicating the complex nature of the adsorption process [26]. Therefore, it can be inferred that adsorption of As(III) onto

Table 2
Pseudo-first-order rate parameters obtained for the sorption of As(III) onto MOCA and AA.

As(III) concentration (mg l^{-1})	MOCA			AA		
	k_1 (h^{-1})	q_e (mg g^{-1})	RMSE	k_1 (h^{-1})	q_e (mg g^{-1})	RMSE
0.95	1.42	0.18	0.005	0.53	0.14	0.004
2.44	1.45	0.44	0.012	0.58	0.37	0.005
4.76	1.50	0.95	0.028	0.59	0.71	0.014
9.98	1.40	1.90	0.071	0.55	1.27	0.049

Table 3
Pseudo-second-order rate parameters obtained for the sorption of As(III) onto MOCA and AA.

As(III) concentration (mg l^{-1})	MOCA			AA		
	k_2 (g mg^{-1} h^{-1})	q_e (mg g^{-1})	RMSE	k_2 (g mg^{-1} h^{-1})	q_e (mg g^{-1})	RMSE
0.95	7.76	0.22	0.004	3.35	0.17	0.003
2.44	3.74	0.50	0.011	1.56	0.44	0.012
4.76	1.60	1.32	0.023	0.83	0.83	0.024
9.98	0.92	2.12	0.026	0.44	1.50	0.021

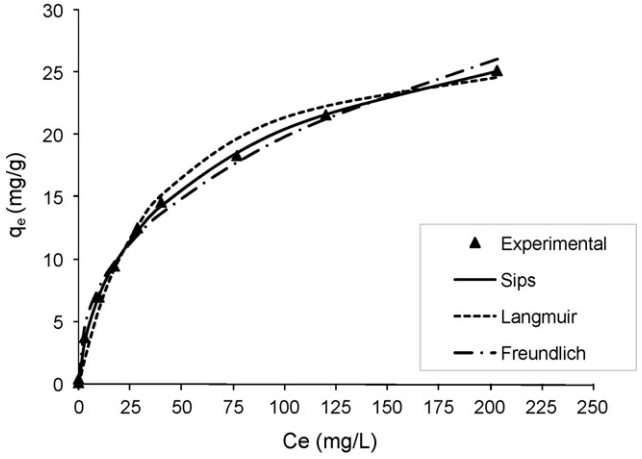

Fig. 5. Comparison of various isotherm plots with experimental equilibrium data for adsorption of As(III) onto MOCA (initial pH = 7 ± 0.2; temperature = 30 ± 1 °C).

MOCA and AA is governed by the combined effect of surface and intraparticle diffusion.

3.2.2. Equilibrium studies

The sorption capacity is one of the basic parameters required for the design of any batch or fixed-bed sorption system. Several sorption isotherm models have been introduced over the years for predicting the sorption capacity of a sorbent. In this study, the equilibrium data obtained for the sorption of As(III) onto AA and MOCA were fitted to Langmuir (L), Freundlich (F) and Sips (S) isotherm models. The mathematical representations of these isotherm models are given in Eqs. (5)–(7).

Langmuir model [27]:

$$q_e = \frac{q_L b_L C_e}{1 + b_L C_e} \quad (5)$$

Freundlich model [28]:

$$q_e = K_F C_e^{1/n} \quad (6)$$

Sips Model [29]:

$$q_e = \frac{q_{mS}(K_S C_e)^{m_S}}{1 + (K_S C_e)^{m_S}} \quad (7)$$

The isotherm plots of adsorption of As(III) onto MOCA are given in Fig. 5 (The corresponding figure for AA is depicted in Fig. 3 of supplementary data). The estimated isotherm parameters obtained from these models are given in Table 4. For both MOCA and AA, the experimental data fitted well to Sips model (three parameter isotherm models), which is evident from the low RMSE value. L model is an analytical equation that assumes monolayer coverage of sorbate over a homogenous sorbent surface [27]. The heterogeneous nature of the sorbents cannot be explained by this model. F model that considers the surface heterogeneity of the sorbents also failed to predict the experimental data well. McKay [30] reported that both L and F theories could not predict the equilibrium data over a wide concentration ranges. Sips model is a three parameter isotherm model (combination of L and F model) developed to improve the performance of L and F model. It is a combination of L and F models having features of both. From the equilibrium sorption studies, it is observed that As(III) sorption onto MOCA is much higher than AA (Table 4). MOCA could remove almost 2 times (42.48 mg g^{-1}) higher As(III) than AA (20.78 mg g^{-1}).

Table 4
Isotherm parameters obtained by fitting equilibrium data with various isotherm models for adsorption of As(III) onto MOCA and AA.

Isotherm models	Model parameters	Adsorbents	
		MOCA	AA
Frendlich	K_F (mg g^{-1}) (mg l^{-1})$^{-1/n}$	3.13	1.43
	$1/n$	0.40	0.45
	RMSE	0.66	0.89
Langmuir	q_{mL} (mg g^{-1})	29.15	19.63
	b_L (l mg^{-1})	0.027	0.019
	RMSE	0.808	0.131
Sips	q_{mS} (mg g^{-1})	42.48	20.78
	K_S (l g^{-1})	0.009	0.017
	m_S	0.65	0.93
	RMSE	0.225	0.076

3.2.3. Effect of co-existing ions on adsorption

Fig. 6(a) and (b) depicts the percentage removal of As(III) by MOCA at various initial concentrations of different co-existing ions. From the figures, it is clear that most of the co-ions studied have shown significant interference on As(III) adsorption by MOCA (over the concentrations range that is normally found in groundwater samples). However, higher concentrations of silicate and bicarbonates have reduced the adsorption efficiency of arsenite. Silicate above 50 mg l^{-1} has shown a negative shift in adsorption efficiency. At 200 mg l^{-1} of silicate, more than 20% reduction in efficiency was observed for an initial As(III) concentration of ~1000 μg l^{-1}. Presence of 200 mg l^{-1} of bicarbonates affected the efficiency of sorption by 5–8%. Occurrence of humic acid (20 mg l^{-1}) has shown around 30% reduction in As(III) removal efficiency. This might be due to the competition of these ions with arsenic for the sorption sites and/or due to masking of sorption sites by the bigger

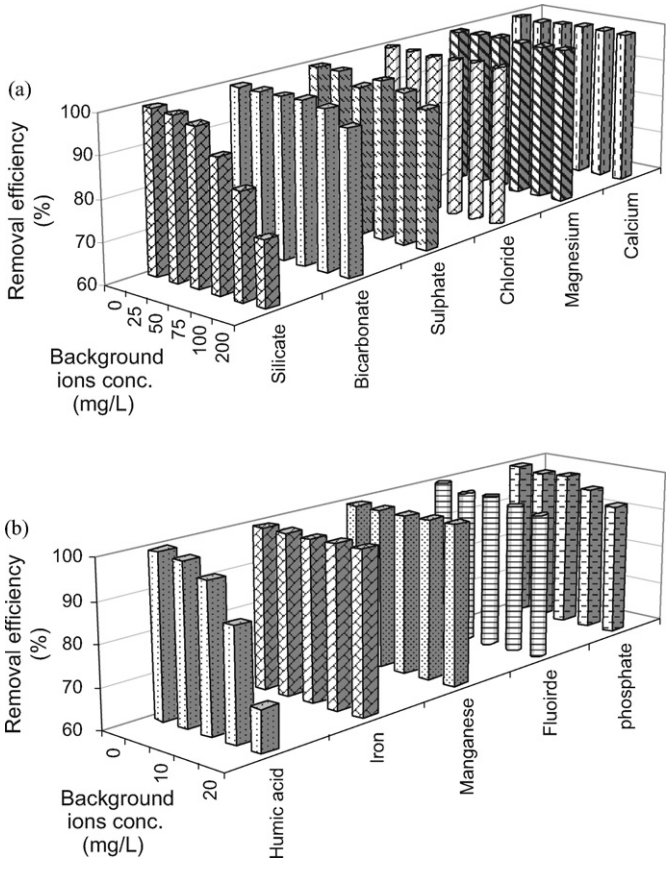

Fig. 6. Effect of various background ions and humic acid on As(III) removal by MOCA (initial As(III) concentration = 1.0 mg l^{-1}; adsorbent dose = 5.0 g l^{-1}; pH = 7 ± 0.2; temperature = 30 ± 1 °C).

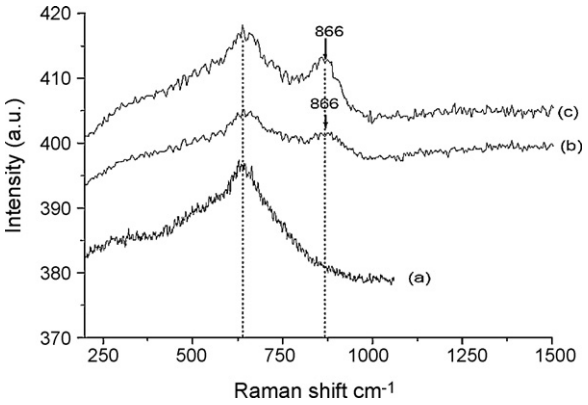

Fig. 7. Raman spectra of (a) virgin MOCA (b) MOCA reacted with As(III) at pH 6 and (c) MOCA reacted with As(III) at pH 8.

humic acid molecules. Phosphate is expected to be a good competing ion for arsenic, since both P and As are located in the same group and have much chemical similarities. Interestingly, in the present study, phosphate (up to 20 mg l^{-1}) has not shown any adverse effect on As(III) sorption by MOCA. This result is in agreement with the findings of Driehaus et al. [5] as per which, As(III) oxidation kinetics and sorption of arsenate was not affected by phosphate.

3.2.4. Mechanism of As(III) sorption onto MOCA

So far, to the best of our knowledge, no research has been performed to understand the interaction of As(III) with manganese oxide coated sorbents. To elucidate the mechanism of As(III) adsorption onto a metal oxide surface, understanding of As-metal oxide bonding is required. Both macroscopic and microscopic experimental methods can give insight into anion sorption mechanisms. In this study, Raman spectroscopy method coupled with sorption experiments were conducted to understand As(III) interaction with MOCA. Fig. 7 shows the Raman spectra of As(III) sorbed MOCA at a pH of 6 and 8 (normal groundwater pH range). From these spectra, the presence of adsorbed As(III) is clearly evident by the presence of the Raman band at 866 cm^{-1}, which corresponds to asymmetric As–O stretching [31]. By varying the pH from 6 to 8, there is no significant shift in the Raman band. This lack of pH dependence on the positions of the Raman band indicate that these modes are "protected" from changes in pH and indicates that these groups are involved in direct complexation with the surface. This data also suggest that, a similar sorption mechanism occurs over this pH range. These results are consistent with the formation of an inner-sphere complex at both pH values [32]. As(III) sorbed AA has not shown any noticeable Raman band that can be attributed to any As(III) surface complexes, at both pH studied. This observation is in agreement with Goldberg and Johnson [32].

Estimation of the effect of ionic strength on adsorption can be used as an indirect method for identifying the mechanism of adsorption [32,33]. According to this method, ions that form outer-sphere surface complexes show decreasing adsorption with increase in ionic strength, whereas ions that form inner-sphere surface complexes show increasing or no variation in adsorption with increase in ionic strength. It was found that, variation in ionic strength had insignificant effect on As(III) sorption onto MOCA, suggesting an inner-sphere surface complex mechanism (data not shown). This can be attributed to the higher activity of the counter ions in the solution available to compensate the surface charge generated by specific ion adsorption [32].

3.2.5. Evidence for the oxidation of As(III) to As(V)

Many researches have shown that oxides of manganese are effective for As(III) to As(V) oxidation. The redox reactions of As(III) with Mn(IV)-oxides and Mn(III)-oxides are [5]:

$$H_3AsO_3 + MnO_2 \leftrightarrow HAsO_4^{2-} + Mn^{2+} + H_2O \quad [E = 0.67\,V] \quad (R1)$$

$$H_3AsO_3 + 2MnOOH + 2H^+ \leftrightarrow HAsO_4^{2-} + 2Mn^{2+} + 3H_2O \quad [E = 0.95\,V] \quad (R2)$$

The measurement of the release pattern of soluble Mn(II) during the redox reaction processes may be used as an indirect evidence for As(III) oxidation to As(V). Fig. 4 in supplementary data shows the Mn(II) release pattern at various initial concentrations of As(III). From the figure, it is evident that soluble Mn(II) is produced during the oxidation reaction of As(III) and an increase in Mn(II) concentration was found with increase in initial As(III) concentrations. Negligible amount of soluble Mn(II) found at low initial As(III) can be attributed to the Mn(II) adsorption capacity of manganese oxide. Driehause et al. [5] has observed a soluble Mn(II) concentration less than 0.2 μmol^{-1} during the oxidation of As(III) (1.3–13.3 μmol^{-1}) and the possible cause for lack of soluble Mn(II) in the system was explained by the high sorption capacity of manganese oxide for soluble Mn(II). Oscarson et al. [34] and Moore et al. [35] have reported that As(V)–manganese complex formation resulted in the absence of soluble Mn(II) in the aqueous phase. However, in the present study, the precipitation of As(V)–manganese complex was not observed.

3.2.6. Effect of pH

In this study, removal efficiency of As(III) by AA and MOCA were evaluated at different pH values. The optimum pH for As(III) removal by AA was between 6.5 and 7.5. However, MOCA could remove As(III) efficiently over a wide pH range of 4–7.5. This variation in optimum pH range might be due to the difference in sorption mechanism of As(III) by AA and MOCA. At pH less than 9.2, H_3AsO_3 is the dominant As(III) species. The specific sorption of a neutral species onto a charged surface like AA is difficult. However, a wider optimum pH range observed for As(III) sorption onto MOCA might be due to the oxidation reaction of initially added As(III) to As(V) and sorption by MOCA. Sorption of soluble Mn(II), released during the oxidation of As(III), by MOCA surface must have compensated the surface charge produced by specific sorption of oxidized As(V). Takamatsu et al. [36] found an increasing amount of As(V) sorption onto manganese oxide with sorption of Mn(II) ions.

As(III) sorption capacity reduced for both AA and MOCA at higher pH (>7.5) values. This may be due to the competition of OH^- ions present in the aqueous solution for sorption sites. The lesser sorption at higher pH values may also be due to the reversal of the surface charges of the sorbents.

3.2.7. Sorbent regeneration

Regeneration of any exhausted adsorbent is an important factor in the sorption process for improving the process economics. In this study, NaOH solution (various concentrations) was used as the eluent for arsenic desorption from exhausted sorbents. It was observed that 2.5% NaOH could elute 88–90% of sorbed arsenic from MOCA.

To test the reusability of regenerated adsorbent, the same sorbent was subjected to three consecutive cycles of adsorption–desorption. The results of these studies (Fig. 8) showed that MOCA have good re-use potential and even at the third cycle, the sorption efficiency was reduced only 5–8%. From the results, it seems that MOCA could be used as an effective alternative sorbent for As(III) removal. However, further investigation is required to get enough information to predict the extent of its applicability in the field.

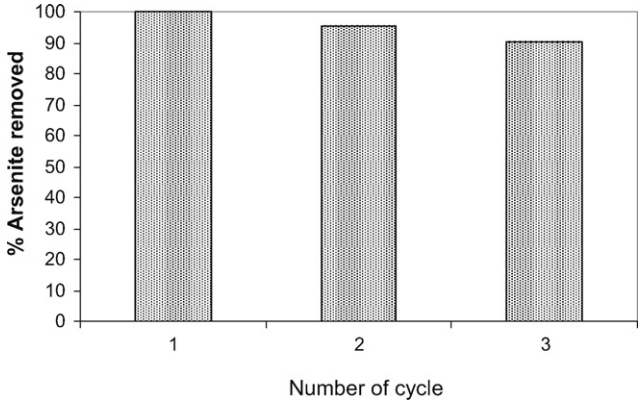

Fig. 8. As(III) removal efficiency of MOCA at three consecutive adsorption cycles (initial As(III) concentration = ~1000 μg l^{-1}; adsorbent dose = 5 g l^{-1}; pH = 7.0 ± 0.2).

4. Conclusions

The As(III) sorption rate and capacity of MOCA was found to be superior to that of AA. The pH conditions of the initial solution influenced the As(III) sorption by both AA and MOCA. The kinetics and equilibrium of sorption onto MOCA were best described by pseudo-second-order equation and Sips isotherm model, respectively. Exhausted MOCA could be regenerated effectively using 2.5% NaOH. The mechanism of As(III) removal by MOCA was found to be a two-step process, i.e. oxidation of As(III) to As(V) and retention of As(V) on MOCA surface, with As(V) forming an inner surface complex with MOCA.

Appendix A. Supplementary data

Supplementary data associated with this article can be found, in the online version, at doi:10.1016/j.cej.2009.06.026.

References

[1] P.H. Masscheleyn, R.D. Delaune, W.H. Patrick, Effect of redox potential and pH on arsenic speciation and solubility in a contaminated soil, Environ. Sci. Technol. 25 (1991) 1414–1419.
[2] EPA, Special Report on Ingested Inorganic Arsenic—Skin Cancer; Nutritional Essentiality, EPA/625/3-87/013F, 124, 1988.
[3] J. Hering, V.Q. Chiu, Arsenic occurrence and speciation in municipal groundwater based supply system, J. Environ. Eng. 126 (5) (2000) 471–474.
[4] M.J. Kim, J. Nriagub, S. Haack, Arsenic species and chemistry in groundwater of southeast Michigan, Environ. Pollut. 120 (2002) 379–390.
[5] W. Driehaus, R. Seith, M. Jekel, Oxidation of arsenite(III) with manganese oxides in water treatment, Water Res. 29 (1995) 297–305.
[6] G. Zhang, J. Qu, H. Liu, R. Liu, R. Wu, Preparation and evaluation of a novel Fe–Mn binary oxide adsorbent for effective arsenate removal, Water Res. 41 (2007) 1921–1928.
[7] EPA, Technologies and Cost for Removal of Arsenic from Drinking Water, EPA Report 815-R-00-012, EPA Office of Water, Washington, D.C., 1999.
[8] P. Mondal, C.B. Majumder, B. Mohanty, Laboratory based approaches for arsenic remediation from contaminated water: recent developments, J. Hazard. Mater. 137 (2006) 464–479.
[9] P. Frank, D. Clifford, As(III) oxidation and removal from drinking water, EPA Project Summary, Report No. EPA/600/S2-86/021, Water Engineering Research Laboratory, Environment Protection Agency, Office of Research and Development, Cincinnati, OH, 1986.
[10] H. Lee, W. Choi, Photocatalytic oxidation of arsenite in TiO_2 suspensions: kinetics and mechanisms, Environ. Sci. Technol. 36 (2002) 3872–3878.
[11] M.J. Scott, J.J. Morgan, Reactions at oxide surfaces: 1. Oxidation of (III) by synthetic birnesite, Environ. Sci. Technol. 29 (1995) 1898–1905.
[12] B.A. Manning, S.E. Fendorf, B. Bostick, D.L. Suarez, Arsenic(III) oxidation and arsenic(V) adsorption reactions on synthetic birnessite, Environ. Sci. Technol. 36 (2002) 976–981.
[13] V. Lenoble, C. Chabroullet, R. Shukry, B. Serpaud, V. Deluchat, J.C. Bollinger, Dynamic arsenic removal on a MnO_2-loaded resin, J. Colloid Interface Sci. 280 (2004) 62–67.
[14] D. Dong, Y.M. Nelson, L.W. Lion, M.S. William, C. Ghiorse, Adsorption of Pd and Cd onto metal oxides and organic material in natural surface coatings as determined by selective extractions: new evidence for the importance of Mn and Fe oxides, Water Res. 34 (2000) 427–436.
[15] S. Kunzru, M. Chaudhuri, Manganese amended activated alumina for adsorption/oxidation of arsenic, J. Environ. Eng. 131 (2005) 1350–1353.
[16] National Environment Protection Council (NEPC), Guideline on Laboratory Analysis of Potentially Contaminated Soils, Schedule B(3) (http://www.ephc.gov.au/pdf/cs/cs_03_lab_analysis.pdf) 1999.
[17] B.M. Babic, S.K. Milonjic, M.J. Polovina, B.V. Kaludierovic, Point of zero charge and intrinsic equilibrium constants of activated carbon cloth, Carbon 37 (1999) 477–481.
[18] F. Kapteijin, A.D. van Langeveld, J.A. Moulijn, A. Andreini, M.A. Vuurman, A.M. Turek, J.M. Jehng, I.E. Wachs, Alumina-supported manganese oxide catalyst. Characterization: effect of precursor and loading, J. Catal. 150 (1994) 94–104.
[19] K.A. Malinger, Y.S. Ding, S. Sithambaram, L. Espinal, S. Gomez, S.L. Suib, Microwave frequency effects on synthesis of cryptomelane-type manganese oxide and catalytic activity of cryptomelane precursor, J. Catal. 239 (25) (2006) 290–298.
[20] J. Hlavay, K. Polyák, Determination of surface properties of iron hydroxide-coated alumina adsorbent prepared for removal of arsenic from drinking water, J. Colloid Interface Sci. 284 (1) (2005) 71–77.
[21] S. Lagergren, Zur theorie der sogenannten adsorption gelöster stoffe, K. Sven, Vetenskapsakad Handl 24 (1898) 1–39.
[22] Y.S. Ho, G. McKay, The kinetics of sorption of divalent metal ions onto sphagnum moss peat, Water Res. 34 (2000) 735–742.
[23] Y.S. Ho, Second-order kinetic model for the sorption of cadmium onto tree fern: a comparison of linear and non-linear methods, Water Res. 40 (1) (2006) 119–125.
[24] L. Axe, P. Trivedi, Intra particle surface diffusion of metal contaminants and their attenuation in microporous amorphous Al, Fe, and Mn oxides, J. Colloid Interface Sci. 247 (2002) 259–265.
[25] W.J. Weber, J.C. Morris, Kinetics of adsorption on carbon from solution, J. Sanit. Eng. Div. ASCE 89 (1963) 31–59.
[26] S.P. Kamble, S. Jagtap, N.K. Labhsetwar, D. Thakare, S. Godfrey, S. Devotta, S.S. Rayalu, Defluoridation of drinking water using chitin, chitosan and lanthanum-modified chitosan, Chem. Eng. J. 129 (2007) 173–180.
[27] L. Langmuir, The adsorption of gases on plane surface of glass, mica and platinum, J. Am. Chem. Soc. 40 (1918) 1361–1403.
[28] H.M.F. Freundlich, Über die Adsorption in Lösungen, Z. Phys. Chem. 57 (1906) 385–470.
[29] R. Sips, Structure of a catalyst surface, J. Chem. Phys. 16 (1948) 490–495.
[30] G. McKay, Kinetics of colour removal from effluent using activated carbon, JSDC 96 (1980) 576–579.
[31] J.A. Tossell, Theoretical studies on arsenic oxide and hydroxide species in minerals and aqueous solution, Geochim. Cosmochim. Acta 61 (1997) 1613–1623.
[32] S. Goldberg, C.T. Johnston, Mechanism of arsenic adsorption on amorphous oxides evaluated using macroscopic measurements, vibrational spectroscopy, and surface complexation modeling, J. Colloid Interface Sci. 234 (2001) 204–216.
[33] Y. Arai, E.J. Elzinga, D.L. Sparks, X-ray absorption spectroscopic investigation of arsenate and arsenate adsorption at the aluminum oxide–water interface, J. Colloid Interface Sci. 235 (2001) 80–88.
[34] D.W. Oscarson, P.M. Huang, W.K. Liaw, U.T. Hammer, Kinetics of oxidation of arsenite by various manganese dioxides, Soil Sci. Soc. Am. J. 47 (1983) 644–648.
[35] J.N. Moore, J.R. Walker, T.H. Hayes, Reaction scheme for the oxidation of As(III) to As(V) by birnessite, Clays Clay Miner. 38 (1990) 549–555.
[36] T. Takamatsu, M. Kawashima, M. Koyoma, The role of Mn2+-rich hydrous manganese oxide in the accumulation of arsenic in lake sediments, Water Res. 19 (1985) 1029–1032.